

Neutron-scattering study of magnetic fluctuations in Zn-substituted $\text{YBa}_2\text{Cu}_3\text{O}_{6.6}$

K. Kakurai

The Institute for Solid State Physics, The University of Tokyo, Roppongi 7-22-1, Minato-ku, 106 Tokyo, Japan

S. Shamoto, T. Kiyokura, and M. Sato

Department of Physics, Nagoya University, Nagoya 464-01, Japan

J. M. Tranquada and G. Shirane

Department of Physics, Brookhaven National Laboratory, Upton, New York 11973

(Received 24 August 1992; revised manuscript received 6 April 1993)

Inelastic-neutron-scattering measurements of magnetic fluctuations in $\text{YBa}_2\text{Cu}_{2.9}\text{Zn}_{0.1}\text{O}_{6.6}$ as a function of temperature are presented. In this nonsuperconducting sample magnetic fluctuations at (π, π) are observed at all temperatures ($10 < T < 200$ K) and energies ($2 < E < 12$ meV) studied in the experiment. This finding should be contrasted to the situation in pure, superconducting $\text{YBa}_2\text{Cu}_3\text{O}_{6.6}$, where the low-energy ($E < 5$ meV) spin fluctuations are suppressed at low temperature leading to gaplike behavior.

INTRODUCTION

To study the nature of the superconductivity in the cuprate superconductors, it is convenient to vary the properties of the CuO_2 planes, the structural elements crucial for the unusual behavior of these materials. In $\text{YBa}_2\text{Cu}_3\text{O}_{6+x}$, the hole doping of the planes can be changed by varying the concentration of oxygen in the CuO chains.¹ Alternatively, one can modify the compounds by substituting other transition metal ions for copper. A particularly interesting dopant is Zn, a nonmagnetic ion which is known to substitute primarily for the planar coppers.^{2,3} While the addition of Zn rapidly suppresses the superconducting transition temperature T_c ,² x-ray absorption studies at the O K edge⁴ have shown that Zn substitution causes little change in the density of hole states (i.e., the reduction of T_c is not simply due to a filling of the holes induced in the planes by the chain oxygens.)

Most studies of Zn doping $\text{YBa}_2\text{Cu}_3\text{O}_{6+x}$ have concentrated on the most highly oxidized material, with $x \sim 1$.² Recently Alloul *et al.*⁵ presented a study of $\text{YBa}_2\text{Cu}_{3-y}\text{Zn}_y\text{O}_{6+x}$ for a fixed y of 0.12 as a function of oxygen content x . Using ^{89}Y nuclear magnetic resonance (NMR) as a probe of local magnetic properties, they established the phase diagram shown in Fig. 1. They also observed that the temperature dependence of the Knight shift of the ^{89}Y line is qualitatively quite similar to that of a pure sample with the corresponding oxygen content. For $x > 0.5$, the main effect of the Zn doping was to induce a line broadening at low temperatures indicative of the formation of static local moments.

A remarkable feature of the Knight shift in both pure and Zn-doped samples with oxygen content x in the range 0.5 to 0.7 is its rapid decrease with decreasing temperature.⁵ A nearly identical temperature dependence is observed in the nuclear spin-lattice relaxation rate measured on ^{17}O in pure sample with $x = 0.63$.⁶ One way of

interpreting this unusual behavior of the spin susceptibility is the formation of a gap in the spin excitations. The anomalous temperature dependence in the Cu spin relaxation rate can be also understood within this picture.⁷ Neutron scattering studies⁸⁻¹¹ have shown that the anomalous variation with temperature of the imaginary part of the spin susceptibility, χ'' , is associated with an energy gaplike structure. Since this magnetic anomalous behavior observed in the Y Knight shift measurement is qualitatively not changed upon Zn doping, which destroys the superconductivity, Alloul *et al.* concluded that the magnetic anomalies are not associated with the superconducting pairing nor superconducting gap.⁵

In this paper we present a neutron scattering study of $\chi''(Q, \omega)$ in a nonsuperconducting single crystal of $\text{YBa}_2\text{Cu}_{2.9}\text{Zn}_{0.1}\text{O}_{6.6}$, and compare with recent results on a pure crystal with the same oxygen content.^{10,11} In contrast to the conclusion drawn from the NMR results,⁵ the

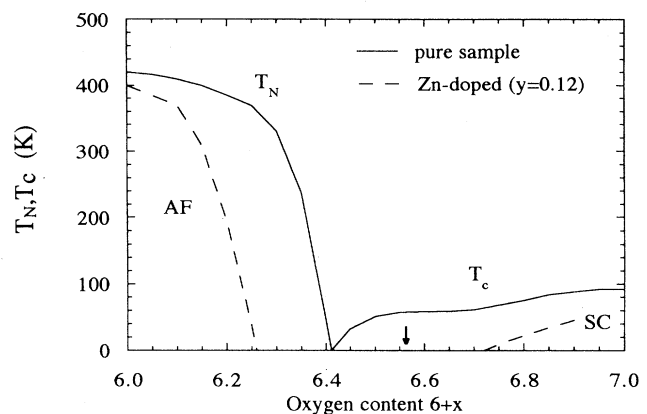


FIG. 1. Schematic T_N and T_c phase diagram of pure and Zn-doped $\text{YBa}_2\text{Cu}_3\text{O}_{6+x}$ (after Ref. 5). The sample used in this experiment is indicated by the arrow.

gaplike structure in the spin fluctuations is completely absent in our Zn-doped crystal; instead, a significant enhancement of χ'' is observed at low frequencies. While the frequency dependence is reminiscent of that in a sample with antiferromagnetic spin correlations over a significant range,¹² the Q width of the inelastic scattering about the antiferromagnetic wave vector is similar to that of the pure sample, indicating the influence of the chain-induced holes. The Zn doping which destroys the superconductivity in our sample clearly has a dramatic effect on the dynamical spin fluctuations.

SAMPLE

The Zn-doped crystal used in this study was grown at Nagoya University by a method described in detail elsewhere.¹³ The only difference was that the cooling rate was reduced (i.e., slower cooling) compared to the previous crystal growths to obtain better quality single crystals. In the starting material Zn to Cu ratio was 0.25 to 2.75. After the crystal growth a part of the single crystal ingot was examined by electron-probe microscopic analysis (EPMA) and the Zn content was determined to be 0.0955. Probably because of the slow cooling rate EPMA indicated also some Al contamination from the Al_2O_3 crucible.

The middle part of the ingot was then annealed at 650°C in the air for seven days together with a pure reference sample. After the anneal the pure sample showed a T_c of 50 K, while the Zn-doped crystal in contrast showed hardly any sign of superconductivity down to 10 K.

To characterize the effects of Zn-doping the lattice constants of the single crystal are compared with the lattice parameters determined using Zn-doped powder sample.¹⁴ The oxygen deficiencies of the powder samples with different Zn doping were determined by measuring the weight losses after quenching from different annealing temperatures. The lattice constants were then determined by powder x-ray diffraction method. The results are summarized in Fig. 2, from which one can conclude that there is little change of the lattice constants caused by Zn doping up to $y=0.12$ at all oxygen contents. The broken lines indicate the earlier results for pure samples.¹⁵ Because the c lattice parameter is known to be insensitive to Al contamination,¹⁶ the oxygen content of the single crystals can be deduced reliably from the c lattice parameter.

The lattice constants of the sample used in this experiment were determined by x-ray powder diffraction to be $a=(3.881\pm 0.003)\text{\AA}$, $b=(3.841\pm 0.003)\text{\AA}$, and $c=(11.733\pm 0.004)\text{\AA}$.

This c parameter corresponds to an oxygen content of 6.56 ± 0.02 , consistent with the oxygen content expected from the annealing condition as mentioned above. The lattice constants of the sample used in this experiment are indicated by shaded circles marked with an arrow in Fig. 2.

To estimate the possible Al contamination we studied the lattice parameters of small pieces taken from the Zn-doped single crystal and heat treated to have different ox-

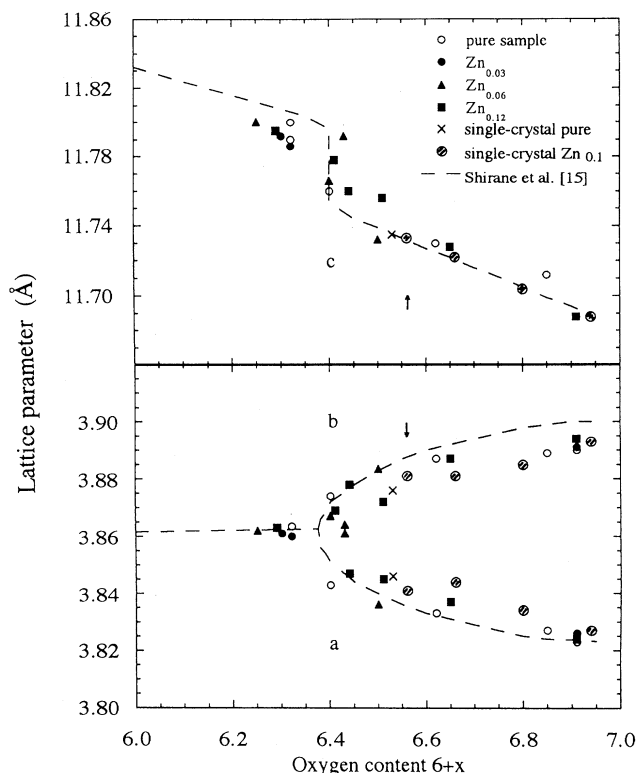


FIG. 2. Lattice constants of $\text{YBa}_2\text{Cu}_{3-y}\text{Zn}_y\text{O}_{6+x}$

xygen contents. The results are indicated by the shaded circles in Fig. 2. As can be seen, the orthorhombicity of the Zn-doped O_{6+x} samples with $0.56 < x < 0.9$ is very close to that of the pure sample. Since the orthorhombicity is known to be very sensitive to the Al contamination,¹⁶ the actual Al contamination in this single crystal is very small indeed.

To check the Zn doping of the single crystal, other physical properties of these differently oxidized crystals were studied. The sample reduced to $\text{O}_{6.1}$ shows antiferromagnetic order with $T_N=370\pm 2$ K. The sample oxygenated to $\text{O}_{6.9}$ becomes superconducting with an onset temperature of 60 K. These findings of the Zn-doped single crystals with different oxidizations are in agreement with the powder phase diagram by Alloul *et al.*⁵ and justifies the direct comparison of the following neutron scattering results with their NMR measurements. The location of our sample in the phase diagram is indicated in Fig. 1 by an arrow.

EXPERIMENT

The experiment was performed on the triple axis spectrometer *H4M* at the High Flux Beam Reactor (HFBR) located at Brookhaven National Laboratory. The (002) reflection of pyrolytic graphite (PG) was used both for the monochromator and analyzer. Scans with different energy transfers and a fixed final energy of $E_f=14.7$ meV were performed. After the sample, a PG filter was used to suppress the higher-order contaminations. Horizontal

collimations were 40'-40'-80'-80'. The sample was oriented with its [110] and [001] axes in the scattering plane. This orientation allows one to scan along and across the two-dimensional (2D) antiferromagnetic (AF) rod, located at $(\frac{1}{2}, \frac{1}{2}, l)$, at different energies.

RESULTS AND DISCUSSION

In Fig. 3 the spectra for fixed energy transfers of 2 to 12 meV at $T=9.5$ K measured across the AF rod are shown. The data are corrected for the systematic normalization error caused by the higher-order contamination seen by the incident beam monitor. These spectra are to be compared to Fig. 1 of Ref. 11. As can be seen there is a striking difference in the low-energy fluctuations between the pure and the Zn-doped sample. While the fluctuations at $E=3$ meV are suppressed in the pure sample, in the Zn-doped sample we can clearly observe strong fluctuations persisting down to the lowest energy transfer of $E=2$ meV.

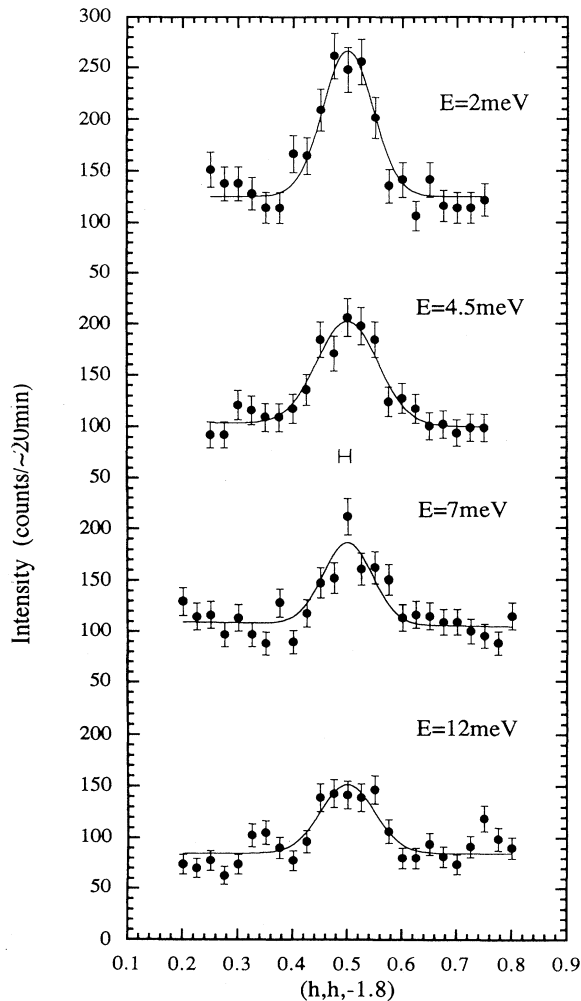


FIG. 3. Constant energy scans at various energies at $T=10$ K along $(h, h, -1.8)$. The solid lines are the results of a fit to a single Gaussian.

In Fig. 4 the intensity modulation along the rod at $E=2$ meV is depicted. This modulation is due to the structure factor of the "acoustic" spin-fluctuation mode caused by the bilayer coupling of the neighboring CuO_2 planes.¹⁷ This clearly indicates that the signal at $E=2$ meV is magnetic and originates from coupled 2D CuO_2 planes.

The solid lines in Fig. 3 are Gaussian fits to the spectra. The horizontal instrumental resolution is indicated by the horizontal bar, and it can be seen that the observed widths are mostly intrinsic. We also checked that the intensity corrections due to the vertical divergence are less than 5%. In what follows we therefore assume that the resolution correction can be neglected.

In Fig. 5 a summary of the Gaussian fit results is given, depicting the maximum intensity (I_{max}) [Fig. 5(a)] and half width at half maximum (HWHM) [Fig. 5(b)] for different temperatures and energies. Figure 5(b) shows that the observed widths are almost independent of the temperatures and energy transfers studied. Therefore the maximum intensities in Fig. 5(a) can be regarded as directly proportional to the temperature- and energy-dependent intensities of magnetic fluctuations,

$$S(\omega) = \int S(q, \omega) dq \propto I_{\text{max}}(\omega).$$

Since the imaginary part of the dynamic susceptibility is related to the integrated intensity by the detailed balance factor, we obtain

$$\chi''(\omega) = S(\omega)(1 - e^{-\hbar\omega/kT}) \propto I_{\text{max}}(\omega)(1 - e^{-\hbar\omega/kT}).$$

It is obvious that at 10 K the dynamic susceptibility in this Zn-doped sample increases with decreasing energy transfer down to 2 meV. This is in contrast to the pure $\text{YBa}_2\text{Cu}_3\text{O}_{6.6}$ behavior, where a gaplike structure in the magnetic excitations is seen.⁹⁻¹¹ To make this clear Fig. 6 shows the energy dependence of χ'' at $T=10$ K. The open and closed points are for the Zn-doped sample and the squares are the data of the pure sample.^{9,10} The normalization of the intensities between the two different sets of data is performed using the intensity of the longitudinal acoustic phonon at $Q=(0,0,6.25)$. The uncertainty of the normalization is of the same order as the error

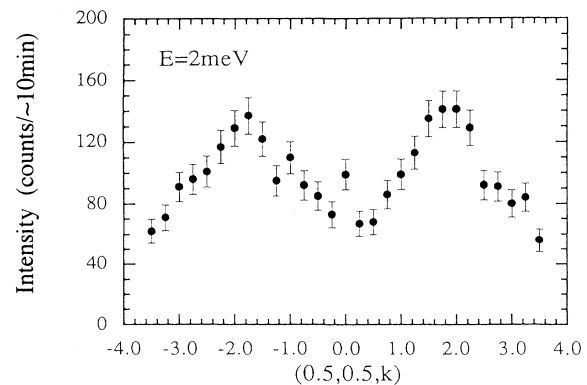


FIG. 4. Constant energy scan at $E=2$ meV at $T=10$ K along $(0.5, 0.5, k)$.

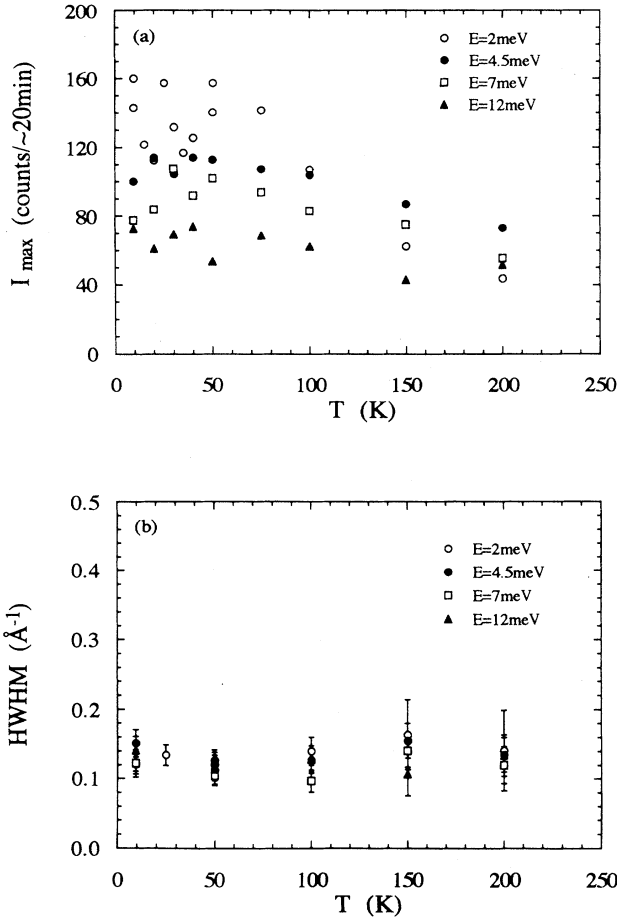


FIG. 5. Summary of the Gaussian fit results. (a) I_{\max} at various energies for different T . (b) HWHM at various energies for different T .

bars. Obviously the quasienergy gap at low T observed in the pure sample disappears upon Zn doping, at the same time as the superconducting property is destroyed. The main weight of the spectrum observed around an energy transfer of 30 meV in the pure sample appears to be shifted towards lower energy in the Zn-doped sample.

This behavior is in contrast to the recent conclusions drawn by Alloul *et al.*⁵ from the NMR Knight shift results. The Knight shift measures the real part of the spin susceptibility for Q and ω equal to zero, $\chi'(0,0)$. Similarities in the temperature dependences of the observed Knight shifts for Y, O, and Cu and nuclear spin-lattice relaxation rates for O and Cu for pure $\text{YBa}_2\text{Cu}_3\text{O}_{6+x}$ have suggested the relationship¹⁸

$$[\chi''(Q,\omega)/\omega]_{\omega \rightarrow 0} \sim \chi'(0,0)g(Q),$$

where the dynamics of antiferromagnetically correlated Cu spins are modeled by the function $g(Q)$. Actually, this form is inconsistent with neutron scattering results on pure samples with reduced oxygen contents, where a gaplike behavior is observed in the frequency dependence of $\chi''(Q,\omega)$, with distinct T dependences above and below the gap energy.⁸⁻¹¹ Nevertheless, the decrease in

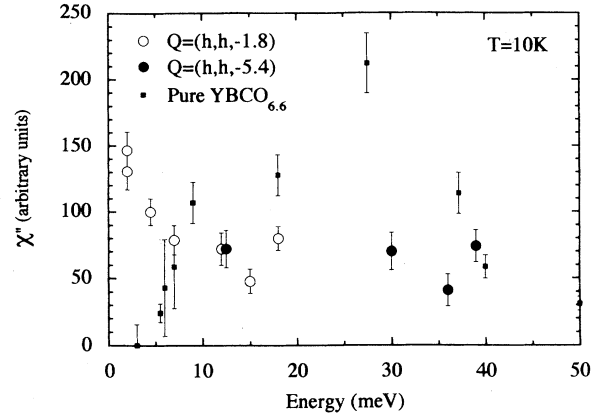


FIG. 6. $\chi''(\omega)$ at $T=10\text{K}$. The squares are the data of the pure $\text{YBa}_2\text{Cu}_3\text{O}_{6.6}$ (Refs. 9 and 10).

$\chi'(0,0)$ at low temperature has become associated with the gaplike behavior observed for $T_c \sim 60\text{K}$ samples. Alloul *et al.*⁵ argue that the similar T dependence of the Y Knight shifts observed for their $x \sim 0.6$ samples with and without Zn doping indicates that the magnetic anomalies such as the spin fluctuation gap are not directly associated with the appearance of superconductivity. To the contrary, our results indicate that the suppression of superconductivity by Zn doping leads to the disappearance of the gaplike behavior and the emergence of strong low-frequency spin fluctuations. This suggests that $\chi'(0,0)$ is an unreliable indicator for anomalies in $\chi''(Q,\omega)$.

It is noteworthy that the Q width of the magnetic scattering in the Zn-doped sample is very similar to the pure sample. The similar Q width of the magnetic scattering in the pure and Zn-doped $\text{O}_{6.6}$ crystals indicates that the typical size of antiferromagnetically correlated regions is the same in the two samples. The Zn-doping causes the increase in low-energy fluctuations without increasing the magnetic correlations. This is different to the pure $\text{O}_{6.4}$ case which shows similar low-energy fluctuations but with markedly larger antiferromagnetic correlations. To understand the origin of the low-energy fluctuations in the Zn-doped sample the temperature and energy dependence of χ'' are considered in more detail.

Recently it has been found that the susceptibility in the normal state of the nearly metallic cuprate systems displays an universal behavior when plotted versus scaled temperatures E/T ,¹⁹⁻²¹ namely

$$\chi''_{2D}(\omega, T) = \chi_0(\omega, 0) \frac{2}{\pi} \tan^{-1} \left[A \frac{\omega}{T} \right], \quad (1)$$

where $\chi_0(\omega, 0)$ is a normalization factor which turns out to be the low-temperature value of χ'' for a given energy transfer.²⁰ The pure $\text{YBa}_2\text{Cu}_3\text{O}_{6.6}$ sample shows a clear deviation from this universal behavior for small energy transfers because of the quasigap structure.¹¹ Figure 7 shows the result of the scaling behavior in the Zn-doped $\text{YBa}_2\text{Cu}_3\text{O}_{6.6}$ sample; fitting the data yields $A = 1.0 \pm 0.1$. Unlike in the pure case the scaling is obeyed over all the

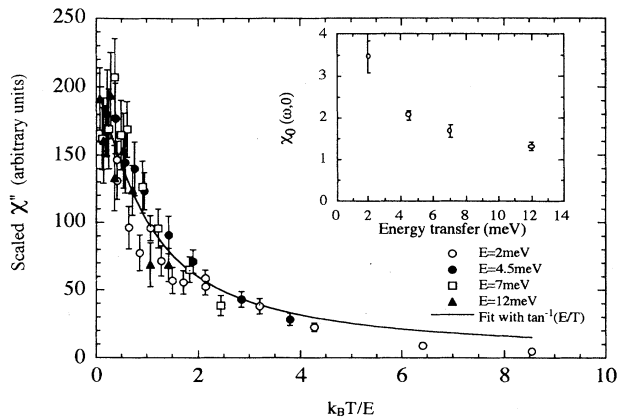


FIG. 7. Scaled χ'' vs T/E . The solid line is the best fit to Eq. (1) with $A=1.0\pm 0.1$. The inset shows the normalization factors $\chi_0(\omega,0)$ used for this scaling.

energy transfers studied. The normalization factor used for this scaling is depicted in the inset. One notes that $\chi_0(\omega,0)$ is enhanced at low energies, qualitatively very similar to the behavior observed in $\text{La}_{1.94}\text{Sr}_{0.06}\text{CuO}_4$ (Ref. 20) and $\text{YBa}_2\text{Cu}_3\text{O}_{6.4}$ (Refs. 12 and 22) in the same energy range, although the enhancement may be less significant in the latter case. Obviously the Zn doping enhances χ'' for small energy transfers as seen in the normal state of the nearly metallic cuprate systems. But the unchanged antiferromagnetic correlation length upon Zn doping as mentioned above indicates that this enhancement in χ'' occurs without reducing the hole concentration in the CuO_2 planes. (The conclusion that the hole concentration is unchanged by the presence of Zn is consistent with x-ray absorption results⁴ and the magnitude of the Y Knight shift.^{5,23}) An effective mechanism must exist to enhance the low-energy spin fluctuations which at the same time leads to the destruction of the superconductivity.

The effectiveness of the nonmagnetic Zn dopants in the CuO_2 plane indicates that this is not merely a diluting effect. The drastic change in the low-energy spin fluctuations suggests that the characteristic electronic structure of the superconducting sample is modified by the randomness introduced by the Zn doping. Two possible physical pictures are suggested.

(a) The quasigap in spin fluctuations is associated with formations of singlet pairing of Cu spins, a prerequisite to the superconducting state within the frame of the mean-field theory based on the t - J model.²⁴ The Zn doping prevents the formations of these singlets and hence eliminates the superconductivity.

(b) The dynamically correlated regions are pinned by the Zn impurities. The pinning leads to a quasistatic component of the correlations which increases with decreasing temperature. The pinning and the slow fluctuations are consistent with the increased linewidth observed in the ^{89}Y NMR study.⁵ Some hints on the physical picture may be obtained by studying the magnetic fluctuations in the Zn-doped sample with different oxygen contents. Neutron scattering studies addressing this issue are under way.

In summary, the above neutron scattering results unequivocally demonstrate that the quasigap behavior in spin fluctuations at (π,π) in the pure, superconducting $\text{YBa}_2\text{Cu}_3\text{O}_{6.6}$ is drastically changed upon Zn doping. The low-energy spin fluctuations are strongly enhanced and thus the quasigap behavior disappears. Because the superconductivity disappears at the same time, a relationship between the anomalous behavior in magnetic fluctuations at (π,π) and the superconductivity is near at hand. This is further supported by the fact that the preliminary results on Zn-doped $\text{YBa}_2\text{Cu}_3\text{O}_{6.6}$ with an onset $T_c=60$ K now under study clearly show a suppression of the low-energy magnetic fluctuations at (π,π) at low T . This finding may seem to contradict the conclusion drawn by Alloul *et al.* from the results of ^{89}Y NMR Knight shift measurements on Zn-doped Y-Ba-Cu-O, but can be understood when the differences between the two methods are considered.

ACKNOWLEDGMENTS

One of the authors (K.K.) would like to thank all the members of the neutron scattering group at BNL for the kind hospitality during his stay. We benefited from discussions with M. Matsuda, B. J. Sternlieb, and T. R. Thurston. This study was supported by the U.S.-Japan Collaborative Program on Neutron Scattering. Work at Brookhaven National Laboratory was carried out under Contract No. DE-AC02-76CH00016, Division of Material Science, U.S. Department of Energy.

¹R. J. Cava, *Science* **247**, 656 (1990).

²L. H. Greene and B. G. Bagley, in *Physical Properties of High Temperature Superconductors II*, edited by D. M. Ginsburg (World Scientific, Singapore, 1990), pp. 509–569.

³H. Maeda, A. Koizumi, N. Bamba, E. Takayama-Muromachi, F. Izumi, H. Asano, K. Shimizu, H. Moriwaki, H. Maruyama, Y. Kuroda, and Y. Yamazaki, *Physica C* **157**, 483 (1989); C. Y. Yang, A. R. Moodenbaugh, Y. L. Wang, Y. Xu, S. M. Heald, D. O. Welch, M. Suenaga, D. A. Fischer, and J. E. Penner-Hahn, *Phys. Rev. B* **42**, 2231 (1990); B. Roughani, L. C. Sengupta, S. Sundaram, and W. C. H. Joiner, *Z. Phys. B*

86, 3 (1992).

⁴M. L. denBoer, C. L. Chang, H. Petersen, M. Schaible, K. Reilly, and S. Horn, *Phys. Rev. B* **38**, 6588 (1988).

⁵H. Alloul, P. Mendels, H. Casalta, J. F. Marucco, and J. Arabski, *Phys. Rev. Lett.* **67**, 3140 (1991).

⁶M. Takigawa, A. P. Reyes, P. C. Hammel, J. D. Thompson, R. H. Heffner, Z. Fisk, and K. C. Ott, *Phys. Rev. B* **43**, 247 (1991).

⁷H. Yasuoka, T. Imai, and T. Shimizu, in *Strong Correlation and Superconductivity*, edited by H. Fukuyama, S. Maekawa, and A. P. Malozemoff (Springer-Verlag, Berlin, 1989).

- ⁸J. Rossat-Mignod, L. P. Regnault, C. Vettier, P. Bourges, P. Burlet, J. Bossy, J. Y. Henry, and G. Lapertot, *Physica C* **185–189**, 86 (1991).
- ⁹P. M. Gehring, J. M. Tranquada, G. Shirane, J. R. D. Copley, R. W. Erwin, M. Sato, and S. Shamoto, *Phys. Rev. B* **44**, 2811 (1991).
- ¹⁰J. M. Tranquada, P. M. Gehring, G. Shirane, S. Shamoto, and M. Sato, *Phys. Rev. B* **46**, 5561 (1992).
- ¹¹B. J. Sternlieb, M. Sato, S. Shamoto, G. Shirane, and J. M. Tranquada, *Phys. Rev. B* **47**, 5320 (1993).
- ¹²H. Chou, J. M. Tranquada, G. Shirane, T. E. Mason, W. J. L. Buyers, S. Shamoto, and M. Sato, *Phys. Rev. B* **43**, 5554 (1991).
- ¹³S. Shamoto, S. Hosoya, and M. Sato, *Solid State Commun.* **66**, 195 (1988).
- ¹⁴H. Harashina, T. Kiyokura, and M. Sato (unpublished).
- ¹⁵G. Shirane, J. Als-Nielsen, M. Nielsen, J. M. Tranquada, H. Chou, S. Shamoto, and M. Sato, *Phys. Rev. B* **41**, 6547 (1990); R. J. Cava, B. Battlog, K. M. Rabe, E. A. Rietman, P. K. Gallagher, and L. W. Rupp, Jr., *Physica C* **156**, 523 (1988).
- ¹⁶J. M. Tarascon, P. Barboux, P. F. Miceli, L. H. Greene, G. W. Hull, M. Eibschutz, and S. A. Sunshine, *Phys. Rev. B* **37**, 7458 (1988).
- ¹⁷J. M. Tranquada, G. Shirane, B. Keimer, S. Shamoto, and M. Sato, *Phys. Rev. B* **40**, 4503 (1989).
- ¹⁸R. E. Walstedt and W. W. Warren, Jr., *Science* **248**, 1082 (1990).
- ¹⁹S. M. Hayden, G. Aeppli, H. Mook, D. Rytz, M. F. Hundley, and Z. Fisk, *Phys. Rev. Lett.* **66**, 801 (1990).
- ²⁰B. Keimer, R. J. Birgeneau, A. Cassanho, Y. Endoh, R. W. Erwin, M. A. Kastner, and G. Shirane, *Phys. Rev. Lett.* **67**, 1930 (1991); B. Keimer, N. Belk, R. J. Birgeneau, A. Cassanho, C. Y. Chen, M. Greven, M. A. Kastner, A. Aharony, Y. Endoh, R. W. Erwin, and G. Shirane, *Phys. Rev. B* **46**, 14034 (1993).
- ²¹R. J. Birgeneau, R. W. Erwin, P. M. Gehring, M. A. Kastner, B. Keimer, M. Sato, S. Shamoto, G. Shirane, and J. M. Tranquada, *Z. Phys. B* **87**, 15 (1992).
- ²²M. Sato, S. Shamoto, T. Kiyokura, K. Kakurai, G. Shirane, B. J. Sternlieb, and J. M. Tranquada, *J. Phys. Soc. Jpn.* **62**, 263 (1993).
- ²³H. Alloul, P. Mendels, G. Collins, and P. Mood, *Phys. Rev. Lett.* **61**, 746 (1988).
- ²⁴H. Fukuyama, *Int. J. Mod. Phys.* (to be published).